HHS Public Access

Author manuscript

Clin Exp Pharmacol Physiol. Author manuscript; available in PMC 2024 January 01.

Published in final edited form as:

Clin Exp Pharmacol Physiol. 2023 March ; 50(3): 247–255. doi:10.1111/1440-1681.13741.

Ablation of TRPC3 compromises bicarbonate and phosphate transporter activity in mice proximal tubular cells

Samuel Shin[1], **Eugenia Awuah Boadi**[1], **Bidhan C. Bandyopadhyay**[1,2]

[1]Calcium Signaling Laboratory, Research Service, Veterans Affairs Medical Center, Washington, Columbia, USA

[2]Division of Renal Diseases & Hypertension, Department of Medicine, The George Washington University, Washington, Columbia, USA

Abstract

Proximal tubular (PT) cells reabsorb most calcium (Ca^{2+}), phosphate (PO_4^{3-}), bicarbonate (HCO_3^-), and oxalate ($C_2O_4^{2-}$) ions. We have shown that mice lacking Transient Receptor Potential Canonical 3 ($TRPC3^{-/-}$) channel are moderately hypercalciuric with presentation of luminal calcium phosphate (CaP) crystals at the loop of Henle (LOH). However, other predisposing factors for such crystal deposition are unknown. Thus, we examined the distinctions in functional status of HCO_3^-, PO_4^{3-}, and $C_2O_4^{2-}$ transporters in PT cells of wild type (WT) and $TRPC3^{-/-}$ mice by whole-cell patch clamp techniques to assess their contribution in the development of LOH CaP crystals. Here we show the development of concentration dependent HCO_3^--induced currents in all PT cells, which was confirmed by using specific HCO_3^- channel inhibitor, S0859. Interestingly, such activities were diminished in PT cells from $TRPC3^{-/-}$ mice, suggesting reduced HCO_3^- transport in absence of TRPC3. While PO_4^{3-}-induced currents were also concentration dependent in all PT cells (confirmed by PO_4^{3-} channel inhibitor, PF-06869206), those activities were reduced in absence of TRPC3, suggesting lower PO_4^{3-} reabsorption that can leave excess luminal PO_4^{3-}. Next, we applied thiosulfate ($O_3S_2^{2-}$) as a competitive inhibitor of the SLC26a6 transporter upon $C_2O_4^{2-}$ current activation and observed a reduced $C_2O_4^{2-}$-induced conductance which was greater in $TRPC3^{-/-}$ PT cells. Together, these results suggest that the reduced activities of HCO_3^-, PO_4^{3-}, and $C_2O_4^{2-}$ transporters in moderately hypercalciuric ($TRPC3^{-/-}$) PT cells can create a predisposing condition for CaP and CaP tubular crystallization, enabling CaP crystal formation in LOH of $TRPC3^{-/-}$ mice.

Correspondence Bidhan C. Bandyopadhyay, Calcium Signaling Laboratory, Research Service, Veterans Affairs Medical Center, Chief, Calcium Signaling Laboratory, 151 Research Service, DCVA Medical Center, 50 Irving Street, NW, Washington, Columbia, 20422, USA. bidhan.bandyopadhyay@va.gov.

AUTHOR CONTRIBUTIONS

All authors contributed to the study conception and design. Material preparation, data collection and analysis were performed by Samuel Shin (SS), Eugenia Awuah Boadi (EAB) and Bidhan C. Bandyopadhyay (BCB). The first draft of the manuscript was written by SS and BCB and all authors commented on previous versions of the manuscript. All authors read and approved the final manuscript. SS performed experiments, analysed data, prepared the figures, and interpreted the results. EAB performed experiments, analysed data, help to prepare the figures, and interpreted the results. BCB designed the concept, interpreted the results, wrote, help to prepared figures, and edited manuscript.

CONFLICTS OF INTEREST

The authors declare no competing financial and/or non-financial interests in relation to the work described in this manuscript.

Keywords

bicarbonate; ion transport; mice; moderate hypercalciuria; oxalate; phosphate; proximal tubule

1 | INTRODUCTION

The proximal tubule (PT) plays a major role in reabsorbing inorganic solutes such as calcium (Ca^{2+}), phosphate (PO_4^{3-}), bicarbonate (HCO_3^-), and oxalate ($C_2O_4^{2-}$) ions, as well as organic solutes such as glucose and amino acids.[1] In addition, the PT is responsible for regulating acid–base balance through bicarbonate resorption and secretion of organic acids.[2] Importantly, PT handles about 65%–70% of the tubular Ca^{2+} load through Ca^{2+} transport,[3] thus being a critical site for preventing Ca^{2+} supersaturation (SS), immediately downstream at the loop of Henle (LOH). Although PT Ca^{2+} reabsorption is usually described as being paracellular (passive), previous studies have shown some evidence of active transport, via transcellular pathway.[4] Importantly, it is twice that of the DCT where Ca^{2+} reabsorption is entirely transcellular.[5] Our efforts to find such transcellular Ca^{2+} transport in the PT revealed the localization of a Ca^{2+} permeable channel, Transient Receptor Potential Canonical 3 (TRPC3), in the apical brush border area, leading to Ca^{2+} entry, and thereby operates transcellular Ca^{2+} reabsorption at this site.[6] Moreover, $TRPC3^{-/-}$ mice exhibited microcalcifications at the luminal region of LOH, thus providing evidence that TRPC3 can contribute to most of the Ca^{2+} entry into PT cells, whereby the absence of TRPC3 significantly raised the PT luminal Ca^{2+}. However, we do not know whether such elevated PT luminal Ca^{2+} in the absence of TRPC3 can directly alter the PT microenvironment and contribute to SS to form calcium phosphate (CaP) microcrystals.

In addition to increases in Ca^{2+}, the ambient pH has a profound effect on the SS of Ca^{2+} and PO_4^{3-} to form CaP, since the crystallization of CaP is strongly favoured by a pH of 6.5 or greater.[7] The solubility of CaP crystals is also pH-dependent and is greatly increased at a pH of 6.2 or less. The PT reabsorbs ~80% of the filtered HCO_3^-, which creates nascent HCO_3^- to neutralize the mineral acids generated by metabolism[8] and thus can play a major role in CaP crystallization. The cells move the HCO_3^- into the interstitial fluid and ultimately to the blood, mainly via the renal splice variant of the electrogenic Na^+/HCO_{3-} co-transporter NBCe1.[8,9] Studies on defective NBCe1 in mice revealed signs of metabolic acidosis and renal tubular acidosis due to bicarbonate wasting, which may increase urinary Ca^{2+} concentration.[10] Moreover, instances of recurrent CaP stone formation have been reported in patients due to renal acidification.[11] However, we do not know how TRPC3 mediated Ca^{2+} can influence HCO_3^- transport in PT cells.

Besides high urinary Ca^{2+} and pH, another important factor that can favour CaP crystallization is high urinary [PO_4^{3-}], which is mostly reabsorbed in the PT.[12] Renal tubular PO_4^{3-} reabsorption is mediated by a sodium gradient–dependent PO_4^{3-} (Na^+/PO_4^{3-}) cotransport system located on the apical brush borders,[13] mainly through the sodium-coupled PO_4^{3-} transporters NaP_i-iia and NaP_i-iic.[14] NaP_i-iia is considered as the main apical PT PO_4^{3-} transporter responsible for up to 70% of the renal PO_4^{3-} reabsorption.[15] Elevated tubular Ca^{2+} leads to the increased urinary SS with respect to both CaP and calcium oxalate

(CaOx), providing the driving force for CaP and/or CaOx nephrolithiasis.[16] In addition to PT Ca^{2+} and PO_4^{3-} transport, $C_2O_4^{2-}$ transport also contributes to mixed stone formation.[17] Thus, optimal regulation of PO_4^{3-} and $C_2O_4^{2-}$ transport should lower the SS of both PO_4^{3-} and $C_2O_4^{2-}$, and inhibit the nucleation of CaP at LOH, a precursor for CaOx stone formation. SLC26A6 expressed in mice PT mediates $C_2O_4^{2-}$ transport in PT cells,[17,18] the absence of which results in the formation of CaOx stones.[18]

An incomplete form of renal PT acidosis has been described in patients with hypercalciuria and stone disease, characterized by abnormal bicarbonaturia.[19] In these patients having transient bicarbonaturia, the presence of other risk factors such as hypercalciuria promotes favourable conditions for the formation of CaP crystals, possibly at the tip of LOH, where luminal pH normally increases to 7.3.[20] PO_4^{3-} intake regulates the reabsorption of renal PO_4^{3-} transport in PT.[21] All of these clinical findings suggest that CaP microcrystal formation at the LOH in our TRPC3$^{-/-}$ mice may be linked to the PT mechanism of pH regulation and PO_4^{3-} transport. We propose that TRPC3 ablation can functionally impact the regulation of HCO_3^- and PO_4^{3-} transport at the PT to drive CaP microcrystal formation at the LOH. Here we presented the functional status of HCO_3^-, PO_4^{3-} and $C_2O_4^{2-}$ transporters in PT cells of WT and TRPC3$^{-/-}$ mice to understand their role in the PT mechanism of regulation of those ion channels in the absence of TRPC3.

2 | MATERIALS AND METHODS

2.1 | Reagents and chemicals

Sodium bicarbonate, disodium phosphate, (S)-3-Chloro-7-(2-(hydroxy-methyl) morpholino)-2-methyl-5-(trifluoromethyl)-1H-pyrrolo[3,2-b] pyridine-6-carbonitrile (PF-06869206), 2-Chloro-N-[[2′-[(cyanoamino) sulfonyl] [1,1′-biphenyl]-4-yl] methyl]-N-[(4-methylphenyl) methyl]-benzamide (S0859), sodium oxalate, and sodium thiosulfate, were purchased from Sigma-Aldrich (St Louis, MO, USA). All the chemicals used in this study were analytical grade. Dulbecco's modified Eagle's medium (DMEM) was purchased from Invitrogen (Carlsbad, CA, USA).

2.2 | Animals

Both wild type (WT) and TRPC3$^{-/-}$ (KO) mice (C57/BL6) were purchased from the Jackson Laboratory (Bar Harbor, ME, USA), were maintained, and crossed as previously described.[6,22] Study design for the mice was approved through a protocol created in accordance with the Guiding Principles in the NIH Care and Use of Animals, approved by the Institutional Animal Care and Use Committee (IACUC) and the Research and Development (R&D) Committee of DC Veterans Affair Medical Center.

2.3 | Primary PT cell isolation

Kidneys from WT and TRPC3$^{-/-}$ mice were extracted, and PT cells were isolated utilizing various techniques adopted in our laboratory as previously described.[6] Once the mice were killed, kidneys were immediately removed and rinsed with an ice-cold standard external saline (SES) buffer (145 mM NaCl, 5 mM KCl, 1 mM $MgCl_2$, 10 mM Na-HEPES, 10 mM glucose; pH 7.4) with 0.02% soybean trypsin inhibitor and 0.1% bovine serum

albumin. Afterwards, kidneys were decapsulated and sliced into coronal sections. Cortical tissues from the kidneys were used to isolate PT cells by enzymatic digestion containing 1% collagenase Type II and 0.25% soybean trypsin inhibitor (Worthington Biochemical Company, Freehold, NJ, USA). Briefly, suspended cells were passed through a 70-micron filter and then resuspended in a 45% Percoll gradient for centrifugation at ~27,000 *g* for 15 min at ~4°C. PT cells were centrifuged and washed for remaining Percoll removal and resuspended in SES or DMEM medium.

2.4 | Electrophysiology

Ion currents were measured using whole-cell patch clamp from freshly isolated single PT cells as previously described.[6] Briefly, cells were bathed in an external solution (140 mM NaCl, 4 mM KCl, 1 mM $MgCl_2$, 2 mM $CaCl_2$, 5 mM D-glucose and 10 mM HEPES; NaOH, pH 7.4) and the intracellular solution (50 mM CsCl, 10 mM NaCl, 60 mM CsF, 20 mM EGTA, and 10 mM HEPES; CsOH, pH 7.2) was also used. Whole-cell current voltage ramp recordings were obtained from an EPC-10 digitally controlled amplifier and Patchmaster software (HEKA, Lambrecht, Germany). *I–V* curves were measured in 3 s intervals, during which voltage ramps were applied from −100 to +100 mV from a holding potential of −80 mV. Data were acquired at 5.00 kHz and filtered at 2.873 kHz. Membrane patch resistance was achieved at >500 MΩ, where resistance was cut-off. Experiments were performed at 25°C. All details about the inclusion and exclusion conditions are described in each corresponding figure legend.

2.5 | RNA extraction and RT-PCR

Total RNA was extracted from WT or TRPC3$^{-/-}$ PT cells using TRIzol reagent as described previously.[6] Afterwards, resultant RNA was treated with DNAse, and concentration of each RNA sample was measured with a nanodrop spectrophotometer. After measuring RNA concentration, a cDNA synthesis kit (Promega, Madison, WI, USA) was used to reverse transcribe the RNA into cDNA, and then amplified with gene specific primers (Table 1) that were purchased from Invitrogen and Integrated DNA Technologies (Coralville, IA, USA) using the PCR master mix amplification reagent (Promega, Madison, WI). T100 Thermocycler (Bio-Rad, Hercules, CA, USA) settings for RT-PCR amplification were set to the specific conditions as described previously[6] with the following PCR conditions: one initial cycle at 95°C for 3 min; 30–35 cycles of denaturation at 95°C for 30 s, annealing at 55°C for 30 s, and elongation at 72°C for 45 s; an additional 5 min at 72°C; and a final hold at 4°C.

2.6 | Protein analysis and western blotting

Cells were washed once in 1xPBS with 1% Aprotinin (Sigma Chemicals, St. Louis, MO, USA) and then solubilised in RIPA buffer with protease inhibitors (Thermo-Fisher Scientific, Waltham, MA, USA) for protein analyses in SDS-PAGE (4%–12%) gels. Protein samples were then transferred into an Immobilon-P^{SQ} transfer membrane (Millipore Corp, Bedford, MA, USA) as previously described.[6] Specific primary antibodies as described in Table 2 were used to label the protein of interest. Horseradish peroxidase (HRP)-conjugated secondary antibodies from Santa Cruz Biotechnology (1:2000 dilution) were utilized to

tag the primary antibodies and enhanced chemiluminescence (ECL) kit (Thermo Scientific Pierce ECL Plus Substrate) was used for HRP signal detection.

2.7 | Statistical analysis

I–V curves were plotted and analysed using Origin 6.1. Statistical analyses were performed using Student's unpaired *t*-test (two-tailed), or ANOVA, as appropriate, in Origin 6.1. The data were expressed as means ± SEM from at least four separate experiments ($n = 4$) as indicated in the figure legends.

3 | RESULTS

3.1 | Functional role of NBCe1 transporter in TRPC3$^{-/-}$ PT cells

Our previous study showed that the TRPC3$^{-/-}$ mice exhibited CaP crystal formation at the LOH with higher urinary Ca^{2+} excretion, which could be linked to the decreased Ca^{2+} reabsorption in the PT.[6] Studies have also shown that higher tubular pH can facilitate the formation of CaP crystals.[23,24] However, it is unclear whether luminal pH changes in the PT can increase the risk for CaP crystal formation at the LOH. It is also known that the handling of HCO_3^- in the PT is crucial for regulating the pH in the luminal fluid.[25] Here we show that the application of sodium bicarbonate in both WT and TRPC3$^{-/-}$ PT cells can develop a current in a concentration dependent manner (Figure 1A,B). Notably, such current response appeared robust in WT PT cells, and the changes were more proportional with the rise in concentration of HCO_3^- from 0.1 mM → 0.3 mM → 1 mM (Figure 1A). Whereas, in TRPC3$^{-/-}$ PT cells, not only was the depth of the current much smaller, but there was almost no change in current density at the lower concentrations (0.1–0.3 mM), suggesting that TRPC3 deletion may affect the current induced by HCO_3^- (Figure 1B) in the PT cells. Since NBCe1 is a major transporter for HCO_3^- regulation in the PT, and that its dysfunction may have an effect on tubular pH,[9,26] we observed the difference between physiological functioning of HCO_3^--induced current activity in presence and absence of TRPC3, using S0859, a selective high-affinity generic inhibitor of NBC.[27] Our results show that the HCO_3^--activated currents in both WT and TRPC3$^{-/-}$ PT cells were significantly diminished (Figure 1C-E), confirming that NBCe1 is involved as the major transporter for HCO_3^- regulation in PT cells. Once again, the pattern of activation in the WT PT cells (Figure 1F) looked much more prominent than the TRPC3$^{-/-}$ PT cells (Figure 1G). However, there was no change in percent inhibition by S0859 between WT and KO PT cells (Figure 1H). To confirm these results, we examined the gene expression for NBCe1 for both WT and TRPC3$^{-/-}$ PT cells. NBCe1 expression levels for gene and protein were insignificant between WT and TRPC3$^{-/-}$ PT cells (Figure 1I,J). These results show that the ablation of TRPC3 may modify the reabsorption activity of HCO_3^- and associated pH regulation in PT cells, while the expression levels remain the same between WT and KO PT cells.

3.2 | Functional role of NaPi-iia in TRPC3 null PT cells

Renal PO_4^{3-} leak due to decreased reabsorption of PO_4^{3-} has been shown to increase the risk of calcium nephrolithiasis.[28] Moreover, most of the renal handling of PO_4^{3-} is managed in the PT.[15] However, whether the increased PO_4^{3-} in the luminal fluid of the PT

contributes to CaP crystal formation at the LOH as seen in our TRPC3$^{-/-}$ mice is unknown. Our recent finding regarding increase in urine CaP crystal formation in TRPC3$^{-/-}$ mice prompted us to examine how it would influence the transport of PO_4^{3-} within TRPC3$^{-/-}$ PT cells.[6] Electrophysiological experiments show a concentration-dependent (0.1–10 mM) induction of currents due to the application of disodium phosphate in WT and TRPC3$^{-/-}$ PT cells (Figure 2A,B). While the pattern of current development with the increase in PO_4^{3-} concentration appeared to be very similar in both WT and TRPC3$^{-/-}$ PT cells, the concentrations between 1–3 mM induced a more prominent current in the TRPC3$^{-/-}$ PT cells than in the WT counterpart (Figure 2A-E). Since the NaP_i-iia co-transporter is the major PO_4^{3-} transporter in the PT for luminal PO_4^{3-} reabsorption in adult mice kidneys,[29] we utilized a selective inhibitor against NaP_i-iia, PF-06869206, to compare the current inhibition between the WT and the TRPC3$^{-/-}$ PT cells.[30] We found that with the application of PF-06869206 in WT PT cells, the PO_4^{3-}-induced current was mildly inhibited (Figure 2F), whereas, such inhibition did not affect the PO_4^{3-}-induced current in TRPC3$^{-/-}$ cells (Figure 2G,H), suggesting that TRPC3-ablated PT cells may experience less PO_4^{3-} uptake through the NaPi-iia than its WT counterpart. Examination of Na-Piia gene and protein expression levels revealed no significant differences between the WT and TRPC3$^{-/-}$ PT mice cells (Figure 2I,J).

3.3 | Thiosulfate diminishes $C_2O_4^{2-}$ induced conductance in PT cells

Recent studies have found that most calcium stones were composed of CaOx with CaP as core component,[31] hence $C_2O_4^{2-}$ transport may be relevant in the present context. The mSLC26a6 transporter was found to be a major $C_2O_4^{2-}$ transporter in the apical region of the PT, where the majority of $C_2O_4^{2-}$ is reabsorbed.[32] Since we have shown that the ablation of TRPC3 in mice increased the amount of CaP formation due to disruption in Ca^{2+} reabsorption in the PT, we wanted to investigate how this ablation may be influencing the $C_2O_4^{2-}$ transport through electrophysiological studies. A previous study has shown thiosulfate ($O_3S_2^{2-}$) to be a potential competitive inhibitor of $C_2O_4^{2-}$ mobilization through SLC26a6, $C_2O_4^{2-}$ transporter, due to its higher affinity.[33] When we first exposed both WT (Figure 3A) and TRPC3$^{-/-}$ PT cells (Figure 3B) to $C_2O_4^{2-}$, there was a rapid development of current, suggesting an increase in the anion exchanger (SLC26a6) activity. We found that the inhibitory pattern via $O_3S_2^{2-}$ in WT PT cells (Figure 3A) mirrors that of TRPC3$^{-/-}$ PT cells (Figure 3B). As we applied $O_3S_2^{2-}$ to the cells, the $C_2O_4^{2-}$-induced conductance was diminished with the rise in concentration (0.1–3 mM) of $O_3S_2^{2-}$ (Figure 3A,B), showing that $O_3S_2^{2-}$ can be a competitive inhibitor via the SLC26a6 ($C_2O_4^{2-}$ transporter) in mouse PT cells, while suggesting a functional presence of $C_2O_4^{2-}$ transport in the PT. Interestingly, at lower concentrations, inhibition by $O_3S_2^{2-}$ was less in WT PT cells and more in TRPC3$^{-/-}$ PT cells, while at the higher concentrations, the inhibition was more prominent in WT than that of the TRPC3$^{-/-}$ PT cells (Figure 3C,D). At the same time, the steepness of the inhibition was greater when applying lesser concentrations (0.1–1 mM) of $O_3S_2^{2-}$ in TRPC3$^{-/-}$ PT cells than in WT PT cells (Figure 3A,B), suggesting the competitive inhibition by $O_3S_2^{2-}$ in such that PT cell oxalate handling might be more tolerant in WT PT cells compared to TRPC3$^{-/-}$ PT cells. The differences in SLC26 gene and protein expression levels between WT and TRPC3$^{-/-}$ mice PT cells were insignificant (Figure 3E,F).

4 | DISCUSSION

Among the major events of renal acid–base homeostasis that occur in the PT, filtered HCO_3^- reabsorption and ammonia generation are prominent. Thus, the regulation of PT HCO_3^- reabsorption through an intracellular pH-independent mechanism can play a role in luminal CaP crystal formation.[34] Our characterization of the anion currents for HCO_3^-, PO_4^{3-}, and $C_2O_4^{2-}$ transporters confirmed those major transporters within WT PT cells to establish the ionic status under normal condition. Moreover, we compared those current activities in TRPC3$^{-/-}$ PT cells to WT PT cells to distinguish the ionic mobilization (by comparing current activity) upon establishing current conductance activity for HCO_3^-, PO_4^{3-} and $C_2O_4^{2-}$. A previous study shows that HCO_3^- activated current in bovine parotid acinar cells were heavily regulated by NBCe1.[35] Our effort was also directed to NBCe1 in the regulation of the HCO_3^- current in PT cells. Since we found NBCe1a is present in PT cells,[6] our results on HCO_3^- current in WT PT cells signifies its functional status.[36] However, in the absence of TRPC3, HCO_3^- current activity was reduced compared to the WT PT cells. Interestingly, mice without AE-1, a bicarbonate-chloride co-transporter, exhibited signs of hypercalciuria, though the actual mechanism has been unclear.[37] While the connection between Ca^{2+} and HCO_3^- regulation has not been well studied in the PT, our study reveals further evidence of how regulation of Ca^{2+} may connect with the regulation of HCO_3^-. Since we did not get robust HCO_3^- response in TRPC3$^{-/-}$ PT cells compared to the WT cells, intracellular HCO_3^- would accumulate which will induce increased NBCe1 activity in an effort to regulate such increased intracellular HCO_3^-, though the expression levels between the WT and KO remained the same (Figure 1I,J). While expression would correlate with activity, a previous study has shown that activity of NBCe1 has increased though expression levels did not change.[9] In the same vein, such increased intracellular HCO_3^- would in turn diminish the luminal secretion of H^+ ions; so that HCO_3^- in PT luminal fluid cannot be neutralized. Such excess HCO_3^- in the tubular fluid can increase the pH, which can explain why we found CaP crystals in the LOH lumen in TRPC3$^{-/-}$ mice.[6]

NaP_i-iia co-transporter knockout mice have been shown to exhibit nephrolithiasis through high phosphate diet.[38] Our previous study has found that there was ~20% increase in PO_4^{3-} excretion in TRPC3$^{-/-}$ mice compared to that of the WT mice,[6] which may be trending towards SS of Ca^{2+} and PO_4^{3-} in TRPC3$^{-/-}$ mice. While the mechanism is unclear, our electrophysiological characterization of the NaP_i-iia transporter current in PT cells revealed that the PO_4^{3-} conductance was significantly inhibited using the NaP_i-iia inhibitor in WT PT cells but not in TRPC3$^{-/-}$ PT cells. This may suggest that NaP_i-iia transporter activity is diminished in the PT of TRPC3$^{-/-}$ mice compared to that of the WT, while less PO_4^{3-} ions is reabsorbed in the PT. Further mechanistic study would be needed to examine the connection between Ca^{2+} and PO_4^{3-} regulation.

Since the most common metabolic abnormality found in calcium stone formers is hypercalciuria, as seen in idiopathic hypercalciuria,[39] we formulated our hypothesis and found that moderately hypercalciuric TRPC3$^{-/-}$ mice presented with CaP crystal formation. It has been proposed that CaP crystals can act as precursor for CaP+CaOx mixed stone formation[40]; in the absence of TRPC3 in PT, such conditions can be used to explore the mechanism of mixed stone formation.[6] We measured the current conductance of murine PT

cells in the presence of $C_2O_4^{2-}$ and show that it has been strongly induced the current both in presence and absence of TRPC3. In both WT and TRPC3$^{-/-}$ PT cells, the conductance has been greatly inhibited, though interestingly, the inhibition has been more prominent in the TRPC3$^{-/-}$ mice cells. A previous study performed with thiosulfate-treated rats revealed decrease in calcium phosphate formation, while in vitro experimentation found that thiosulfate only minimally decreased the ionisation of free calcium, suggesting an inherent mechanism involving thiosulfate in the rats.[41] We show that thiosulfate has a mechanistic influence upon the current activity in PT cells. Since TRPC3$^{-/-}$ PT mice exhibited increase in CaP crystal formation in the urine, future studies can examine if thiosulfate can alleviate the risk of stone formation in these mice.

Additional mechanisms other than NBCe1 appear to regulate PT acid–base regulation such as citrate, which we plan to examine in our future study. NBCe1 expression is detectable only in the proximal convoluted tubule and proximal straight tubule in the renal cortex in normal mice (Diagram 1). We extracted the cortical PT cells to measure the currents, suggesting its validity. We have used pharmacological agents for our study, which may have some off-target effect. Nonetheless, at present, we do not have sufficient data to identify the mechanisms of pH- regulated predisposition of CaP crystal formation in vivo. Future studies along this line using siRNA inhibitor can pin-point the mechanistic output.

5 | CONCLUSION

In summary, our study provides substantial new information on PT status of HCO_3^-, PO_4^{3-}, and $C_2O_4^{2-}$ ion transports in a moderately hypercalciuric condition (Diagram 1) and can advance our understanding of calcium stone formation. Such functional activity may be necessary for generating predisposing condition in TRPC3$^{-/-}$ mice under both basal conditions and in response to metabolic acidosis. Our study provides fundamental knowledge for using TRPC3 ablated mice as an in vivo cellular signalling model to understand the calcium nephrolithiasis and chronic kidney disease involving oxidative stress or crystal nephropathies.

FUNDING INFORMATION

We acknowledge the funding support from National Institute of Diabetes and Digestive and Kidney Diseases (DK102043) to BCB. This funding agencies were not involved in the preparation of the article, study design, collection, analyses, and interpretation of data, writing of the report, or decision to submit this article for publication.

DATA AVAILABILITY STATEMENT

The data that support the findings of this study are available from the corresponding author upon reasonable request.

REFERENCES

1. Zhuo JL, Li XC. Proximal nephron. Compr Physiol. 2013;3:1079–1123. [PubMed: 23897681]
2. Hamm LL, Nakhoul N, Hering-Smith KS. Acid-Base Homeostasis. Clin J Am Soc Nephrol. 2015;10:2232–2242. [PubMed: 26597304]

3. Friedman PA, Gesek FA. Cellular calcium transport in renal epithelia: measurement, mechanisms, and regulation. Physiol Rev. 1995;75:429–471. [PubMed: 7624390]
4. Ullrich KJ, Rumrich G, Klöss S. Active Ca^{2+} reabsorption in the proximal tubule of the rat kidney. Dependence on sodium- and buffer transport. Pflugers Arch. 1976;364:223–228. [PubMed: 986634]
5. White KE, Gesek FA, Nesbitt T, Drezner MK, Friedman PA. Molecular dissection of Ca2+ efflux in immortalized proximal tubule cells. J Gen Physiol. 1997;109:217–228. [PubMed: 9041450]
6. Ibeh CL, Yiu AJ, Kanaras YL, et al. Evidence for a regulated Ca^{2+} entry in proximal tubular cells and its implication in calcium stone formation. J Cell Sci. 2019;132:jcs225268. [PubMed: 30910829]
7. Berg C, Tiselius HG. The effect of pH on the risk of calcium oxalate crystallization in urine. Eur Urol. 1986;12:59–61. [PubMed: 3948899]
8. Boron WF. Acid-base transport by the renal proximal tubule. J Am Soc Nephrol. 2006;17:2368–2382. [PubMed: 16914536]
9. Kurtz I, Zhu Q. Structure, function, and regulation of the SLC4 NBCe1 transporter and its role in causing proximal renal tubular acidosis. Curr Opin Nephrol Hypertens. 2013;22:572–583. [PubMed: 23917030]
10. Alexander RT, Cordat E, Chambrey R, Dimke H, Eladari D. Acidosis and urinary calcium excretion: insights from genetic disorders. J Am Soc Nephrol. 2016;27:3511–3520. [PubMed: 27468975]
11. Goldfarb DS. A woman with recurrent calcium phosphate kidney stones. Clin J Am Soc Nephrol. 2012;7:1172–1178. [PubMed: 22595827]
12. Bushinsky DA, Parker WR, Asplin JR. Calcium phosphate supersaturation regulates stone formation in genetic hypercalciuric stone-forming rats. Kidney Int. 2000;57:550–560. [PubMed: 10652032]
13. Murer H, Lötscher M, Kaissling B, Levi M, Kempson SA, Biber J. Renal brush border membrane Na/pi-cotransport: molecular aspects in PTH-dependent and dietary regulation. Kidney Int. 1996;49:1769–1773. [PubMed: 8743494]
14. Breusegem SY, Takahashi H, Giral-Arnal H, et al. Differential regulation of the renal sodium-phosphate cotransporters NaPi-IIa, NaPi-IIc, and PiT-2 in dietary potassium deficiency. Am J Physiol Renal Physiol. 2009;297:F350–F361. [PubMed: 19493963]
15. Blaine J, Chonchol M, Levi M. Renal control of calcium, phosphate, and magnesium homeostasis. Clin J Am Soc Nephrol. 2015;10:1257–1272. [PubMed: 25287933]
16. Coe FL, Favus MJ, Pak CYC, Parks JH, Preminger GM, eds. Kidney Stones: Medical and Surgical Management. Lippincott Williams & Wilkins; 1996.
17. Ratkalkar VN, Kleinman JG. Mechanisms of stone formation. Clin Rev Bone Miner Metab. 2011;9:187–197. [PubMed: 22229020]
18. Jiang Z, Asplin JR, Evan AP, et al. Calcium oxalate urolithiasis in mice lacking anion transporter Slc26a6. Nat Genet. 2006;38:474–478. [PubMed: 16532010]
19. Antón FM, Puig JG, Caspar G, Martínez ME, Ramos T, Piñeiro JM. Renal tubular acidosis in recurrent renal stone formers. Eur Urol. 1984;10:55–59. [PubMed: 6698089]
20. Brenner B, Hamm L, Nakhoul N. Renal acidification mechanisms. In: Brenner B, ed. Brenner and Rector's the Kidney. Elsevier; 2008:248–279.
21. Chang AR, Anderson C. Dietary phosphorus intake and the kidney. Annu Rev Nutr. 2017;37:321–346. [PubMed: 28613982]
22. Hartmann J, Dragicevic E, Adelsberger H, et al. TRPC3 channels are required for synaptic transmission and motor coordination. Neuron. 2008;59:392–398. [PubMed: 18701065]
23. Siener R, Netzer L, Hesse A. Determinants of brushite stone formation: a case-control study. PLoS One. 2013;8:e78996. [PubMed: 24265740]
24. De Rooij JF, Heughebaert JC, Nancollas GH. A ph study of calcium phosphate seeded precipitation. J Colloid Interface Sci. 1984;100:350–358.
25. Curthoys NP, Moe OW. Proximal tubule function and response to acidosis. Clin J Am Soc Nephrol. 2014;9:1627–1638. [PubMed: 23908456]

26. oye AM, Parker MD, Daly CM, et al. The human NBCe1-a mutant R881C, associated with proximal renal tubular acidosis, retains function but is mistargeted in polarized renal epithelia. Am J Physiol Cell Physiol. 2006;291:C788–C801. [PubMed: 16707554]
27. Ch'en FF, Villafuerte FC, Swietach P, Cobden PM, Vaughan-Jones RD. S0859, an N-cyanosulphonamide inhibitor of sodium-bicarbonate cotransport in the heart. Br J Pharmacol. 2008;153:972–982. [PubMed: 18204485]
28. Prié D, Ravery V, Boccon-Gibod L, Friedlander G. Frequency of renal phosphate leak among patients with calcium nephrolithiasis. Kidney Int. 2001;60:272–276. [PubMed: 11422761]
29. Forster IC, Hernando N, Biber J, Murer H. Proximal tubular handling of phosphate: a molecular perspective. Kidney Int. 2006;70:1548–1559. [PubMed: 16955105]
30. Filipski KJ, Sammons MF, Bhattacharya SK, et al. Discovery of orally bioavailable selective inhibitors of the sodium-phosphate cotransporter NaPi2a (SLC34A1). ACS Med Chem Lett. 2018;9:440–445. [PubMed: 29795756]
31. Tiselius HG. A hypothesis of calcium stone formation: an interpretation of stone research during the past decades. Urol Res. 2011;39:231–243. [PubMed: 21246193]
32. Soleimani M SLC26 Cl-/HCO3- exchangers in the kidney: roles in health and disease. Kidney Int. 2013;84:657–666. [PubMed: 23636174]
33. Landry GM, Hirata T, Anderson JB, et al. Sulfate and thiosulfate inhibit oxalate transport via a dPrestin (Slc26a6)-dependent mechanism in an insect model of calcium oxalate nephrolithiasis. Am J Physiol Renal Physiol. 2016;310:F152–F159. [PubMed: 26538444]
34. Zhou Y, Zhao J, Bouyer P, Boron WF. Evidence from renal proximal tubules that HCO3- and solute reabsorption are acutely regulated not by pH but by basolateral HCO3- and CO2. Proc Natl Acad Sci U S A. 2005;102:3875–3880. [PubMed: 15728388]
35. Yamaguchi S, Ishikawa T. Electrophysiological characterization of native Na+-HCO3- cotransporter current in bovine parotid acinar cells. J Physiol. 2005;568:181–197. [PubMed: 16037094]
36. Kurtz I NBCe1 as a model carrier for understanding the structure-function properties of Na^+ —coupled SLC4 transporters in health and disease. Pflugers Arch. 2014;466:1501–1516. [PubMed: 24515290]
37. Mumtaz R, Trepiccione F, Hennings JC, et al. Intercalated cell depletion and vacuolar H^+-ATPase Mistargeting in an Ae1 R607H Knockin model. J Am Soc Nephrol. 2017;28:1507–1520. [PubMed: 27932475]
38. Li Y, Caballero D, Ponsetto J, et al. Response of Npt2a knockout mice to dietary calcium and phosphorus. PLoS One. 2017;12:e0176232. [PubMed: 28448530]
39. Worcester EM, Coe FL. New insights into the pathogenesis of idiopathic hypercalciuria. Semin Nephrol. 2008;28:120–132. [PubMed: 18359393]
40. Tiselius H-G, Lindbäck B, Fornander A-M, Nilsson M-A. Studies on the role of calcium phosphate in the process of calcium oxalate crystal formation. Urol Res. 2009;37:181–192. [PubMed: 19444436]
41. Asplin JR, Donahue SE, Lindeman C, Michalenka A, Strutz KL. Bushinsky DA thiosulfate reduces calcium phosphate nephrolithiasis. J Am Soc Nephrol. 2009;20:1246–1253. [PubMed: 19369406]

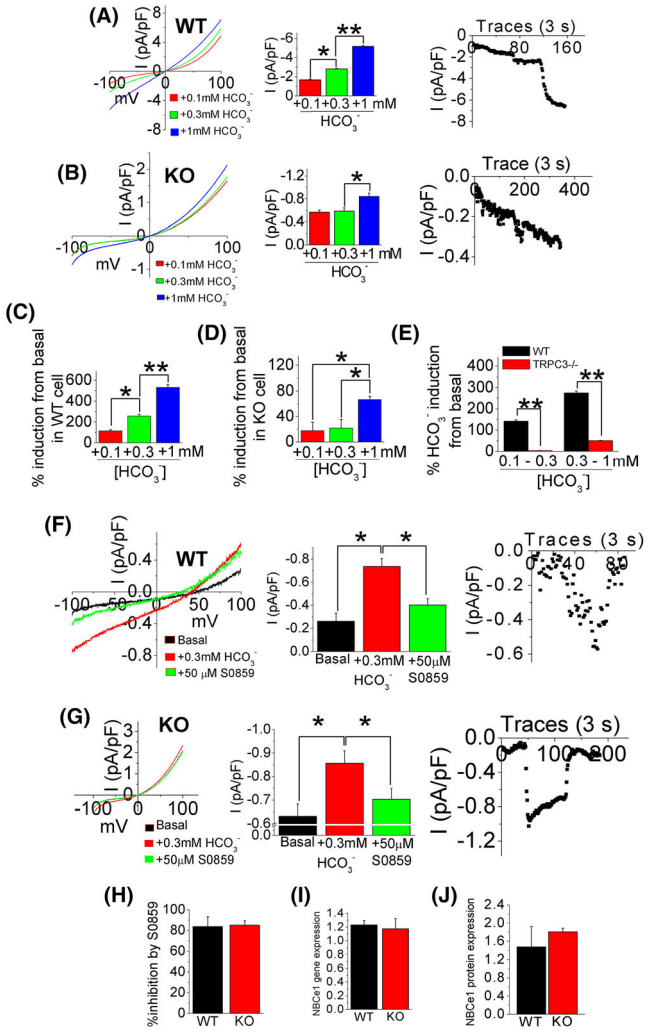

FIGURE 1.

Bicarbonate-activated current is suppressed in WT and TRPC3$^{-/-}$ PT cells after S0859 application. I-V curve recordings and current voltage ramp traces at −100 mV of (A) WT and (B) TRPC3$^{-/-}$ (KO) PT cells of each HCO_3^- concentration dependent application were plotted. (A, B) Bar diagrams depict current densities (pA/pF) at −100 mV in PT cells (WT and KO) which were obtained from WT and KO mice (*n = 4*). (A) For the WT PT cell, sodium bicarbonate (HCO_3^-) was applied at traces 20 (+0.1 mM), 66 (+0.3 mM) and 115 (+1 mM). (B) For KO PT cell, (HCO_3^-) was applied at traces 10 (+0.1 mM), 75 (+0.3 mM), and 150 (+1 mM). Percent induction of basal current densities of (C) WT and (D) KO PT cells were derived from graphs A and B by dividing each current density of implemented HCO_3^- concentration (0.1, 0.3, and 1 mM) from the basal current density. (E) Change in percent HCO_3^- induction (0.1–0.3, and 0.3–1 mM) from basal current densities in WT and KO PT cells was calculated from C and D by subtracting percent current induction at 0.1 mM from 0.3, and 0.3 mM from 1 mM. (F, G) NBCe1 inhibitor, S0859 (50 μM), was applied to WT or KO PT mice cells to inhibit the current activated by (HCO_3^-). (F) Sodium bicarbonate (0.3 mM) was applied at trace 20 and S0859 (50 μM) was applied at trace 60. (G) Sodium bicarbonate (0.3 mM) was applied at trace 55 and S0859 (50 μM)

was applied at trace 61. (F, G) Bar diagrams show current densities (pA/pF) in PT cells (WT and KO) which were obtained from WT and KO mice ($n = 4$). (H) Percent inhibition of HCO_3^- induced current were assessed from F and G by subtracting current densities of WT or KO PT cells after application of S0859 inhibitor, from current density after initial HCO_3^- application. Densitometric analyses of (I) *NBCe1* RT-PCR expression and (J) NBCe1 expression by western blot were quantified using ImageJ from PT cells (WT and KO) of each WT and KO mice ($n = 4$). (A–J) Bar diagrams are represented in mean + SEM. * $P < 0.05$; ** $P < 0.01$

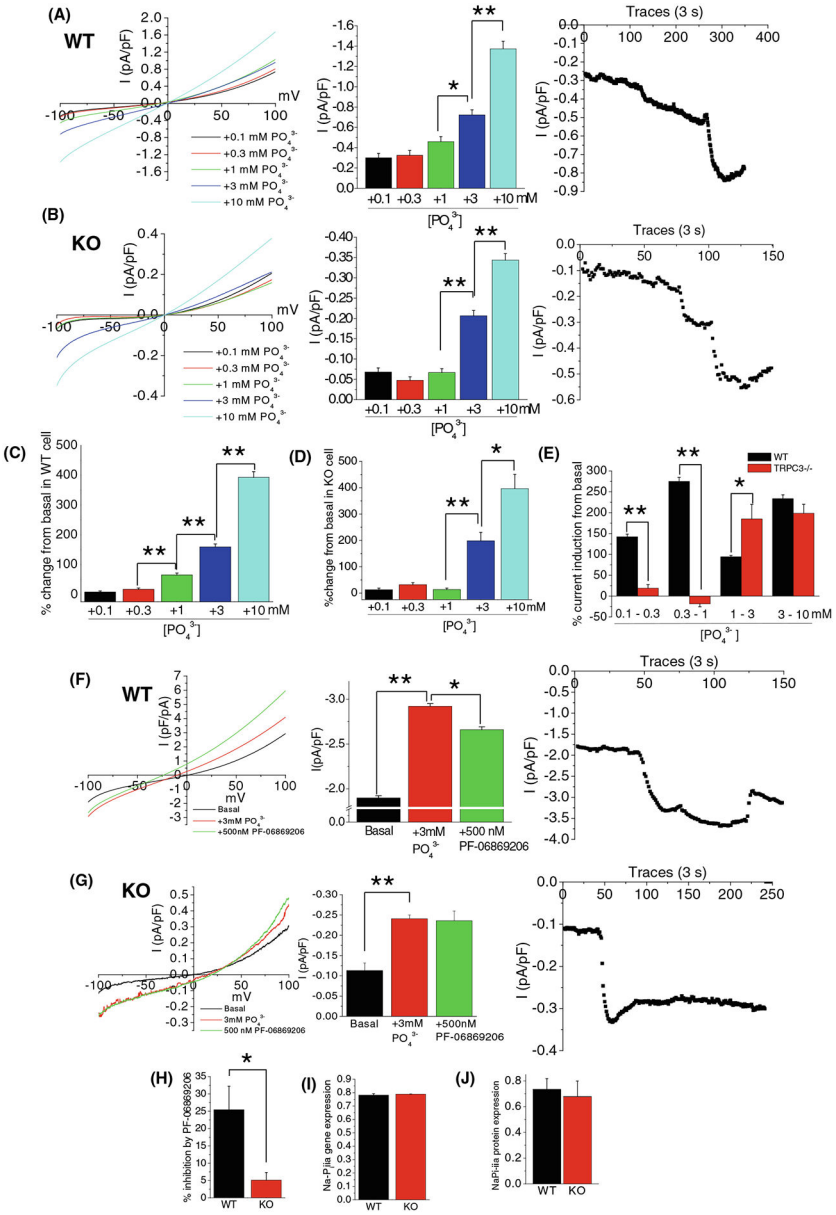

FIGURE 2.

Phosphate-activated current in TRPC3$^{-/-}$ mice was not inhibited by PF-06869206 application. I-V curve recordings of current voltage ramp traces at −100 mV of (A) WT and (B) TRPC3$^{-/-}$ (KO) PT cells of each disodium phosphate concentration dependent applications were plotted. (A, B) Bar diagrams depict current densities (pA/pF) at −100 mV in PT cells (WT and KO) which were obtained from WT and KO mice (*n = 4*). (A) For WT PT cells, disodium phosphate was applied at traces 10 (+0.1 mM), 30 (+0.3 mM), 100 (1 mM), 150 (3 mM), and 250 (+10 mM). (B) For KO PT cells, disodium phosphate was applied at traces 10 (+0.1 mM), 30 (+0.3 mM), 50 (+1 mM), 74 (+3 mM), and 99 (+10 mM). Percent change in induction of current densities in (C) WT and (D) KO PT cells were derived from graphs A and B by dividing each current density of implemented phosphate (PO_4^{3-}) concentration (0.1, 0.3, 1, 3, and 10 mM) from the basal current density.

(E) Change in percent PO_4^{3-} induction (0.1–0.3, 0.3–1, 1–3, and 310 mM) from basal current densities in WT and KO PT cells was calculated from C and D by subtracting percent current induction at 0.1 mM from 0.3 mM, and 0.3 mM from 0.1 mM, 1 mM from 3 mM, and 3 mM from 10 mM. (F, G) NaP_i-iia inhibitor, PF-06869206 (500 nM), was applied to inhibit the current activated by disodium phosphate (3 mM). (F) For WT PT cells, disodium phosphate was applied at trace 47 and PF-06869206 was applied at trace 110. (G) For KO PT cells, disodium phosphate was applied at trace 45 and PF-06869206 was applied at trace 100. (H) Percent inhibitions of PO_4^{3-} induced current were assessed from F and G by subtracting current densities of WT or KO PT cells after application of PF-06869206 inhibitor, from current density after initial PO_4^{3-} application. (F, G) Bar diagrams show current densities (pA/pF) in PT cells (WT and KO) which were obtained from WT and KO mice ($n = 4$). Densitometric analyses of (I) *Na-P_i-iia* RT-PCR expression and (J) Na-P_i-iia expression (western blot) were quantified using ImageJ from PT cells (WT and KO) of each WT and KO mice ($n = 4$). (A–J) Bar diagrams are represented in mean + SEM. *. $P < 0.05$; **, $P < 0.01$

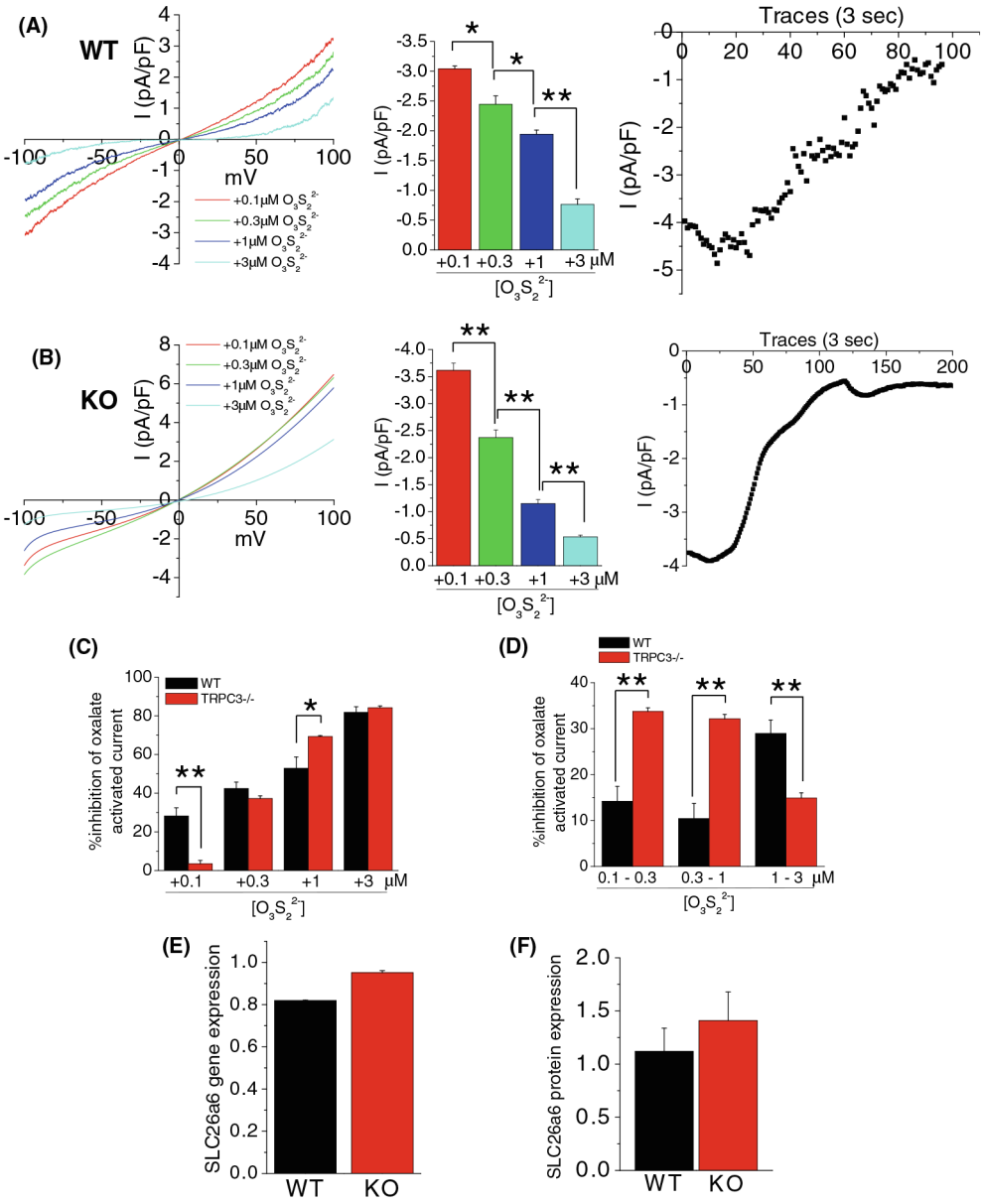

FIGURE 3.

Sodium oxalate induced current was inhibited in a concentration dependent manner in PT cells. Whole-cell patch clamp of (A) WT and (B) TRPC3$^{-/-}$ (KO) PT cells with voltage ramps from −100 to +100 mV in the presence of 100 μM $C_2O_4^{2-}$ were applied $O_3S_2^{2-}$ in a concentration-dependent manner. (A, B) Bar diagrams depict current densities (pA/pF) at −100 mV in PT cells (WT and KO) which were obtained from WT and KO mice (*n = 4*). (A) For WT PT cells, $O_3S_2^{2-}$ was applied at traces 15 (+0.1 mM), 21 (+0.3 mM), 30 (+1 mM), and 60 (+3 mM). (B) For KO PT cells, $O_3S_2^{2-}$ was applied at traces 10 (+0.1 mM), 25 (+0.3 mM), 35 (+1 mM), and 55 (+3 mM). (C, D) Percent inhibitions of $C_2O_4^{2-}$ induced current were assessed from A and B by subtracting current densities of WT or KO PT cells after each application of $O_3S_2^{2-}$, from current density induced by $C_2O_4^{2-}$. I-V curve recordings current voltage ramp traces at −100 mV of each $O_3S_2^{2-}$ application were plotted.

Densitometric analyses of (E) *SLC26a6* RT-PCR expression and (F) SLC26a6 expression by western blot were quantified using ImageJ from PT cells (WT and KO) of each WT and KO mice ($n = 4$)

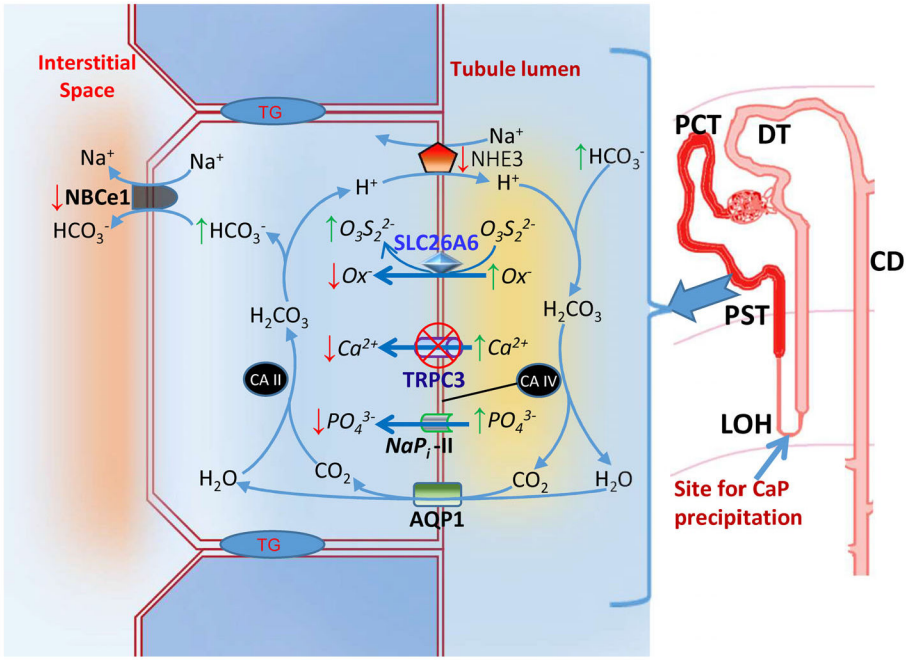

DIAGRAM 1.

Schematic represents ionic regulation in PT cells from TRPC3$^{-/-}$ mice. TRPC3 regulates luminal [Ca^{2+}] rise, NBCe1 handle the pH via carbonic anhydrase (CA). Elevated [Ca^{2+}] in tubular lumen maybe linked to the altered physiology of other solute transporters in PT cells. NaPi-II = Pi transporter regulates PO_4^{3-} Conc.; SLC26A6 = Oxalate transporter regulates PO_4^{3-} Conc.; NBCe1 = Na+/HCO^{3-} co-transporter; NHE3 = Na^+/H^+ exchanger. CD, collecting duct; DT, distal tubule; LOH, loop of henle; PCT, proximal convoluted tubule; PST, proximal straight tubule.

TABLE 1

Primer table

Primer	Sequence (sense, antisense)	Product Size (bp)
mNBCe1	5′-CACTGAAAATGTGGAAGGGAA-3′ 5′-TTATCACCCTTGTGCTTTGC-3′	544
mNaP$_i$-iia	5′-AGACACAACAGAGGCTTC-3′ 5′-CACAAGGAGGATAAGACAAG-3′	181
mSLC26a	5′-AGATCTTCCTTGCGTCTGC-3′ 5′-GCCTTTCCACATGGTAGTCTC-3′	150
mGAPDH	5′-TGAGGACCACGTTGTCTCCT-3′ 5′-GCCCCTCCTGTTATTATGGG-3′	303

TABLE 2

Antibody information

Antibody	Ref. No.	Protein	Dilution	Company
Rabbit polyclonal antibody	11885-1-AP	NBCe1	1:1000	Proteintech
Rabbit polyclonal antibody	NBP2-13328	NaPi2a	1:1000	Novus Biologicals
Mouse monoclonal antibody	sc-515230	SLC26a6	1:1000	Santa Cruz Biotechnology